

Supplementary Information

A High-Performance Non-fullerene Electron Acceptor with Bisalkylthiophene π -Bridges for Organic Photovoltaics

Zhaolong Wang,^{†,#} Kunxiang Huang,^{‡,#} Xianjie Chen,[†] Yating Xu,[†] Zheng Xu,[§] Tian He,[†] Shouchun Yin,[†] Huayu Qiu,^{*,†,§} Miaomiao Li,^{*,‡} Qian Zhang^{*,†}

[†]College of Materials, Chemistry and Chemical Engineering, Hangzhou Normal University, Hangzhou, 311121, P. R. China.

[‡]School of Materials Science and Engineering and Tianjin Key Laboratory of Molecular Optoelectronic Science, Tianjin University, Tianjin 300072, P. R. China.

[§]Key Laboratory of Organosilicon Chemistry and Materials Technology of Ministry of Education, Hangzhou Normal University, Hangzhou 311121, P. R. China.

[#]These authors contributed equally to this paper.

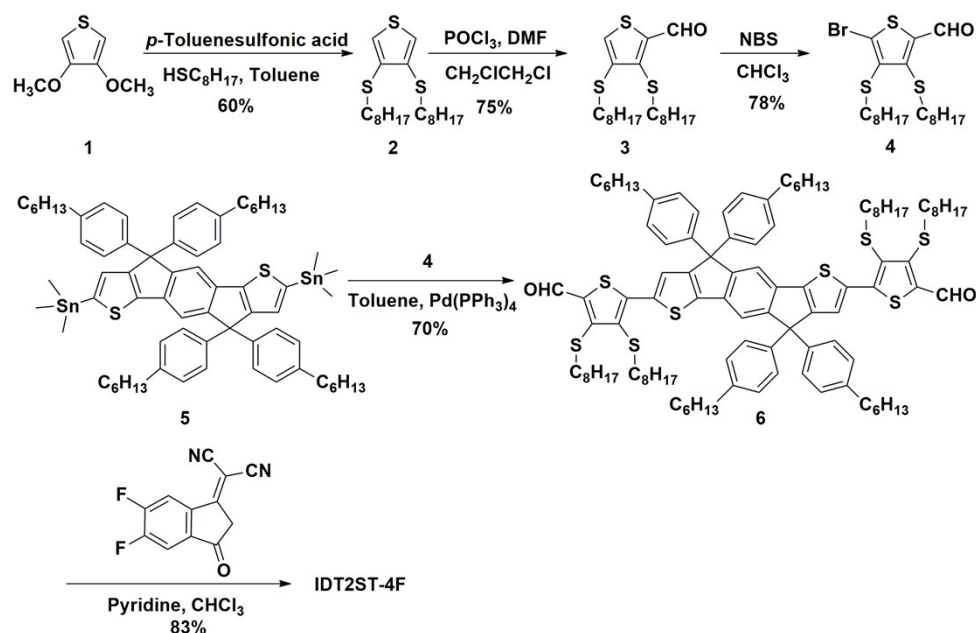
Contents

1. Materials and synthesis.....	4
2. Instruments and general methods	6
3. Solar cell fabrication and characterization	7
4. Supplementary data	8
Fig. S1 ¹ H NMR spectrum of compound 2	9
Fig. S2 ¹³ C NMR spectrum of compound 2	9
Fig. S3 ¹ H NMR spectrum of compound 3	10
Fig. S4 ¹³ C NMR spectrum of compound 3	10
Fig. S5 ¹ H NMR spectrum of compound 4	11
Fig. S6 ¹³ C NMR spectrum of compound 4	11
Fig. S7 ¹ H NMR spectrum of compound 6	12
Fig. S8 ¹³ C NMR spectrum of compound 6	12
Fig. S9 MALDI-TOF mass spectrum of compound 6	13
Fig. S10 ¹ H NMR spectrum of IDT2ST-4F.....	13
Fig. S11 ¹³ C NMR spectrum of IDT2ST-4F.....	14
Fig. S12 MALDI-TOF mass spectrum of IDT2ST-4F.....	15
Fig. S13 (a) TGA and (b) DSC curves of IDT2ST-4F.....	15
Fig. S14 Cyclic voltammogram of IDT2ST-4F in dichloromethane with 0.1 mol L ⁻¹ n-Bu ₄ NPF ₆ at a scan rate of 100 mVs ⁻¹	16
Fig. S15 (a) Electron density distributions of HOMO and LUMO orbitals, and (b) the optimized geometry of IDT2ST-4F with ethyl groups in replacing alkyl substituents to simplify the calculations.....	16
Fig. S16 Chemical structure of PDINO.....	17
Photovoltaic performance	17
Fig. S17 Statistical histogram of PCEs for IDT2ST-4F-based devices (over 20 devices for each case under the as-cast or TA-treated conditions).....	17
Fig. S18 Absorption spectra of the as-cast or TA-treated pristine IDT2ST-4F films (a) and PBDB-T:IDT2ST-4F films (b).....	18

Fig. S19 Dependence of V_{oc} on the light intensity (P_{light}) of the TA-treated IDT2ST-4F-based devices.	19
Fig. S20 (a) In-plane and (b) out-of-plane XRD pattern of the as-cast and TA-treated IDT2ST-4F film.	19
Fig. S21 $J-V$ characteristics of the hole-only (a) and electron-only (b) devices based on the PBDB-T:IDT2ST-4F blend films under different conditions.	19
References	20

1. Materials and synthesis

All reagents and solvents were purchased from commercial sources and used without further purification unless stated otherwise. 3,4-Dimethoxythiophene **1**, (4,4,9,9-tetrakis(4-hexylphenyl)-4,9-dihydro-*s*-indaceno[1,2-*b*:5,6-*b'*]dithiophene-2,7-diyl)bis(trimethylstannane) **5**, and the end-capping groups were purchased from SunaTech Inc. Compounds **2**, **3** and **4** were synthesized according to the literature.¹ PBDB-T (number-average molecular weight: 25.0 kDa, polydispersity index: 2.36) and PDINO were purchased from Solarmer Materials and SunaTech Inc, respectively.



Scheme S1 Synthetic routes to the bisalkylthiophene-based π bridge and IDT2ST-4F.

Compound 2: A mixture of 3,4-dimethoxythiophene **1** (2.5 g, 17.3 mmol) with 5 equivalents of 1-mercaptooctane (12.69 g, 86.5 mmol) and a catalytic amount of *p*-toluenesulfonic acid (0.2 g) in dry toluene (50 mL) was stirred for 16 h at 80 °C under a flow of nitrogen. After cooling down, toluene was removed under reduced pressure and the residue was diluted with water (200 mL). The mixture was extracted with dichloromethane (100 mL \times 2) and the organic layer was washed with dilute NaHCO₃ aqueous solution and brine, dried over anhydrous MgSO₄. The solvent was removed by rotary evaporation and subsequently dried in a vacuum oven. The crude product was purified by column chromatography on silica gel using

dichloromethane/petroleum ether (1:10, v/v) to afford **2** as a colorless liquid (2.4 g, 60%). ¹H NMR (500 MHz, CDCl₃) δ (ppm): 7.11 (s, 2H), 2.91 – 2.86 (t, *J* = 7.4 Hz, 4H), 1.66 (m, 4H), 1.49 – 1.39 (m, 4H), 1.29 (m, 16H), 0.90 (t, *J* = 6.9 Hz, 6H). ¹³C NMR (126 MHz, CDCl₃) δ (ppm): 133.99, 122.89, 34.42, 31.83, 29.20, 29.18, 29.02, 28.84, 22.67, 14.11.

Compound 3: POCl₃ (4 mL) was added dropwise to DMF (1 mL) at 0 °C with the protection of argon. The solution turned into a glue and the color turned into light yellow after stirred for 30 min at room temperature. Then a solution of **2** (1 g, 2.7 mmol) in dry 1,2-dichloroethane (CH₂ClCH₂Cl, 30 mL) was added to the mixture quickly. After stirred and refluxed for 16 h at 70 °C with the protection of argon, the reaction mixture was cooled to room temperature and washed with brine. Then the solution was extracted with dichloromethane (100 mL × 2) and dried over anhydrous MgSO₄. The solvent was removed by rotary evaporation, and the crude product was purified by column chromatography on silica gel using dichloromethane/petroleum ether (1:20, v/v) to afford **3** as a pale-yellow oil (800 mg, 75%). ¹H NMR (500 MHz, CDCl₃) δ (ppm): 10.16 (d, *J* = 1.2 Hz, 1H), 7.28 (d, *J* = 1.1 Hz, 1H), 2.86 (m, 4H), 1.68 – 1.56 (m, 2H), 1.51 – 1.42 (m, 2H), 1.42 – 1.34 (m, 2H), 1.33 – 1.27 (m, 2H), 1.27 – 1.11 (m, 16H), 0.81 (t, *J* = 6.9 Hz, 6H). ¹³C NMR (126 MHz, CDCl₃) δ (ppm): 184.34, 145.12, 140.95, 140.48, 127.68, 36.30, 33.75, 31.79, 31.76, 29.66, 29.16, 29.14, 29.05, 28.90, 28.76, 28.52, 22.64, 22.62, 14.09, 14.08.

Compound 4: A solution of **3** (2 g, 5.0 mmol) in dichloromethane (40 mL) was stirred at 0 °C while *n*-bromosuccinimide (NBS) (0.98 g, 5.5 mmol) was added portion-wise. The reaction mixture was raised to room temperature and maintained at this temperature for 16 h. Then the mixture was poured into ice water (200 ml) and extracted with CH₂Cl₂ (100 mL × 2), dried over anhydrous MgSO₄. The solvent was removed by rotary evaporation. The crude product was purified by column chromatography on silica gel using dichloromethane/petroleum ether (1:10, v/v) as eluant to afford **4** as a pale-yellow oil (1.8 g, 78%). ¹H NMR (500 MHz, CDCl₃) δ (ppm): 10.09 (s, 1H), 2.94 (t, *J* = 7.3 Hz, 2H), 2.82 (t, *J* = 7.3 Hz, 2H), 1.50 – 1.43 (m, 4H), 1.36 – 1.28 (m, 4H), 1.25 – 1.44 (m, 16H), 0.80 (t, *J* = 6.9 Hz, 6H). ¹³C NMR (126 MHz, CDCl₃) δ (ppm): 183.20, 145.42, 144.89, 138.72, 130.97, 36.99, 35.81, 31.79, 31.75, 29.62, 29.59, 29.16, 29.14, 29.12, 29.05, 28.61, 28.55, 22.64, 22.62, 14.09, 14.08.

Compound 6: A solution of **5** (2 g, 1.6 mmol) and **4** (3.8 g, 8 mmol) in dry toluene (100 ml) was degassed twice with argon following the addition of Pd(PPh₃)₄ (0.9 g, 0.8 mmol). After stirred and refluxed for 24 h at 110 °C with the protection of argon, the reaction mixture was poured into water (100 mL) and extracted with CH₂Cl₂ (100 mL x 2). The organic layer was washed with water for twice and dried over anhydrous MgSO₄. After removal of the solvent, the crude product was purified by silica gel using dichloromethane/petroleum ether (1:1) as eluant to afford **6** as a red solid (1.90 g, 70%). ¹H NMR (500 MHz, CDCl₃) δ (ppm): 10.12 (s, 2H), 7.51 (s, 2H), 7.43 (s, 2H), 7.10 (d, *J* = 8.3 Hz, 8H), 7.01 (d, *J* = 8.3 Hz, 8H), 2.92 (t, *J* = 7.4 Hz, 4H), 2.82 – 2.70 (t, *J* = 7.5 Hz, 4H), 2.57 – 2.40 (t, *J* = 7.8 Hz, 8H), 1.66 – 1.37 (m, 20H), 1.27 – 1.05 (m, 50H), 0.87 – 0.70 (m, 24H). ¹³C NMR (126 MHz, CDCl₃) δ (ppm): 183.91, 155.90, 154.10, 149.47, 147.80, 145.50, 141.85, 141.31, 140.46, 137.33, 135.59, 131.61, 128.49, 127.82, 124.36, 118.03, 62.99, 37.30, 36.93, 35.59, 31.75, 31.37, 29.64, 29.27, 28.88, 28.62, 22.62, 14.10. MS (MALDI-TOF): calcd for C₁₀₆H₁₄₂O₂S₈ [M⁺] 1703.8809; found:1703.8848.

IDT2ST-4F: **6** (0.57 g, 0.3 mmol) and 2-(5,6-difluoro-3-oxo-2,3-dihydro-1*H*-inden-1-ylidene)malononitrile **7a** (0.21 g, 0.9 mmol) was dissolved in a dry CHCl₃ (50 ml) solution under the protection of argon, and then three drops of pyridine were added to the mixture. After stirred at room temperature for 16 h, the mixture was extracted with CHCl₃ (50 ml x 2), and the organic layer was washed with water and dried over anhydrous MgSO₄ for 3 h. After removal of the solvent, the crude product was purified by silica gel using dichloromethane/petroleum ether (1:10) as eluant to afford **IDT2ST-4F** (0.59 g, 83%) as a black solid. ¹H NMR (500 MHz, CDCl₃) δ (ppm): 9.44 (s, 2H), 8.49 (m, 2H), 7.72 (s, 2H), 7.61 (t, *J* = 7.5 Hz, 2H), 7.48 (s, 2H), 7.13 (d, *J* = 8.3 Hz, 8H), 7.04 (d, *J* = 8.4 Hz, 8H), 3.00 – 2.91 (t, *J* = 7.5 Hz, 4H), 2.86 – 2.75 (t, *J* = 7.5 Hz, 4H), 2.57 – 2.45 (t, *J* = 7.8 Hz, 8H), 1.60 – 1.45 (m, 20H), 1.35 – 1.19 (m, 40H), 1.19 – 1.10 (m, 30H), 0.78 (m, 24H). ¹³C NMR (126 MHz, CDCl₃) δ (ppm): 186.02, 158.61, 156.96, 154.87, 153.98, 148.10, 142.02, 140.98, 137.80, 136.63, 135.98, 134.74, 133.56, 128.60, 127.92, 125.53, 122.35, 118.36, 114.88, 114.51, 113.88, 112.73, 112.57, 70.65, 63.07, 35.62, 31.80, 31.75, 31.41, 29.20, 29.17, 29.16, 29.16, 29.12, 29.11, 28.92, 28.80, 22.65, 22.62, 22.61, 14.13, 14.10. MS (MALDI-TOF): calcd for C₁₃₀H₁₄₆F₄N₄O₂S₈ [M⁺] 2129.1; found: 2128.9.

2. Instruments and general methods

¹H-NMR and ¹³C-NMR spectra were recorded on a Bruker AVANCE 500 spectrometer. Mass spectra (MS) were recorded on a Walters MALDI Q-TOF Premier mass spectrometry. Thermogravimetric analysis (TGA) and differential scanning calorimetric (DSC) measurements were carried out on a TA Q500 and a NETZSCH DSC 214 instrument under nitrogen gas flow with a 10 °C min⁻¹ heating rate, respectively. UV-vis absorption spectra were obtained with double-beam Hitachi UH5300 spectrophotometer. Cyclic voltammetry (CV) measurements were conducted with the films on the glassy carbon working electrode in dry dichloromethane solution via a LK2005A electrochemical workstation. All CV measurements were carried out at room temperature with a conventional three-electrode configuration employing a glassy carbon electrode as the working electrode, a saturated calomel electrode (SCE) as the reference electrode, and a Pt wire as the counter electrode. Tetrabutylammonium phosphorus hexafluoride (Bu₄NPF₆, 0.1 M) in dichloromethane was used as the supporting electrolyte, and the scan rate was 100 mV s⁻¹. E^{ox}_{onset} and E^{re}_{onset} are oxidation and reduction onsets, respectively, against the half potential of ferrocene/ferrocenium (Fc/Fc⁺), as determined in CV curves. The HOMO and LUMO energy levels were estimated by the equations: HOMO = - (4.8 + E^{ox}_{onset}) eV, LUMO = - (4.8 + E^{re}_{onset}) eV, respectively. Atomic force microscopy (AFM) measurements were carried out in tapping mode on a Bruker MultiMode 8 atomic force microscope. Out-of-plane XRD was measured with a Bruker D8 Advance using CuK α radiation (λ = 1.54056 Å) and operated at 40 kV and 30 mA, and in-plane XRD was conducted on a Rigaku Smart Lab with CuK α source (λ = 1.54056 Å).

3. Solar cell fabrication and characterization

The devices with an architecture of glass/ITO/PEDOT:PSS (40 nm)/PBDB-T:acceptor /PDINO/Al (100 nm) were fabricated. The ITO coated glass substrates were cleaned ultrasonically with detergent, deionized water, acetone and isopropanol under ultrasonication for 15 min each. The dried ITO was treated with UV-ozone for 20 min, and then solution of PEDOT:PSS (Baytron P AI 4083) was spin-coated (ca. 40 nm thick) onto the surface. The substrates were then placed into an argon-filled glove box after being baked at 150 °C for 20 min. Subsequently, the active layer was spin-coated from donor and acceptor mixture in chloroform solution on the ITO/PEDOT:PSS substrate. Subsequently, the substrate was annealed at 110 °C for 5 min. Then PDINO in CH₃OH (1 mg/mL), was spin-coated at 3000 rpm for 40 s on the

active layers. Finally, a 100 nm Al layer was deposited on the PDINO layer under high vacuum ($< 1.5 \times 10^{-4}$ Pa). The effective area of each cell is 4 mm², as defined by masks for the solar cell devices. Keithley 2400 source meter was used to measure J - V curves under 100 mW cm⁻² AM 1.5G simulated solar light illumination provided by an AAA solar simulator (SS-F5-3A, Enli Technology Co. Ltd) calibrated with a standard photovoltaic cell equipped with a KG5 filter in a glove box. The EQE data were obtained using a solar cell spectral response measurement system (QE-R, Enli Technology Co. Ltd).

Hole-only devices with an architecture of ITO/PEDOT:PSS (40 nm)/ PBDB-T:acceptor/Au (100 nm) and electron-only devices with an architecture of glass/Al (100 nm)/PBDB-T:acceptor/Al (100 nm) were fabricated. The devices were measured using Keithley 2400 source meter in a glove box under dark. The hole and electron mobilities were calculated by fitting the dark current using the Mott-Gurney relationship:

$$J = \frac{9}{8} \epsilon_0 \epsilon_r \mu \frac{V^2}{L^3}$$

where J is the current density, L is the film thickness of the active layer, μ is the hole or electron mobility, ϵ_r is the relative dielectric constant of the transport medium, ϵ_0 is the permittivity of free space (8.85×10^{-12} F m⁻¹), V ($= V_{\text{appl}} - V_{\text{bi}}$) is the internal voltage in the device, where V_{appl} is the applied voltage to the device and V_{bi} is the built-in voltage due to the relative work function difference of the two electrodes.

4. Supplementary data

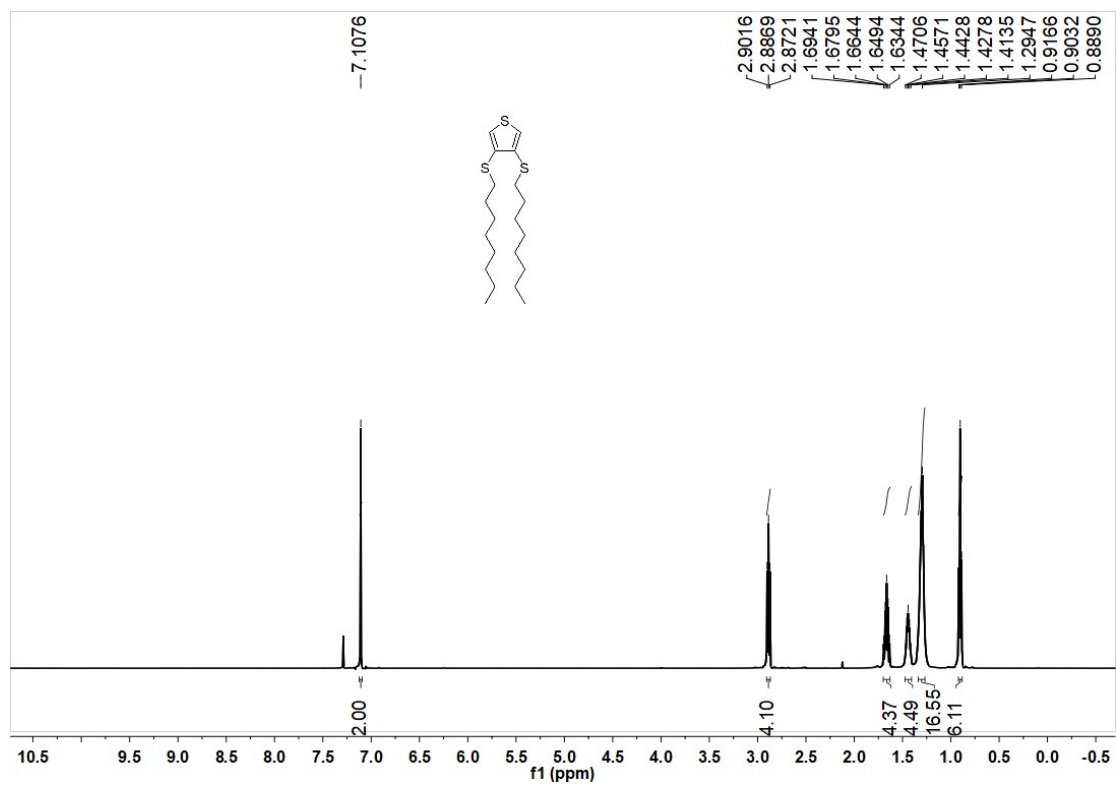


Fig. S1 ^1H NMR spectrum of compound 2.

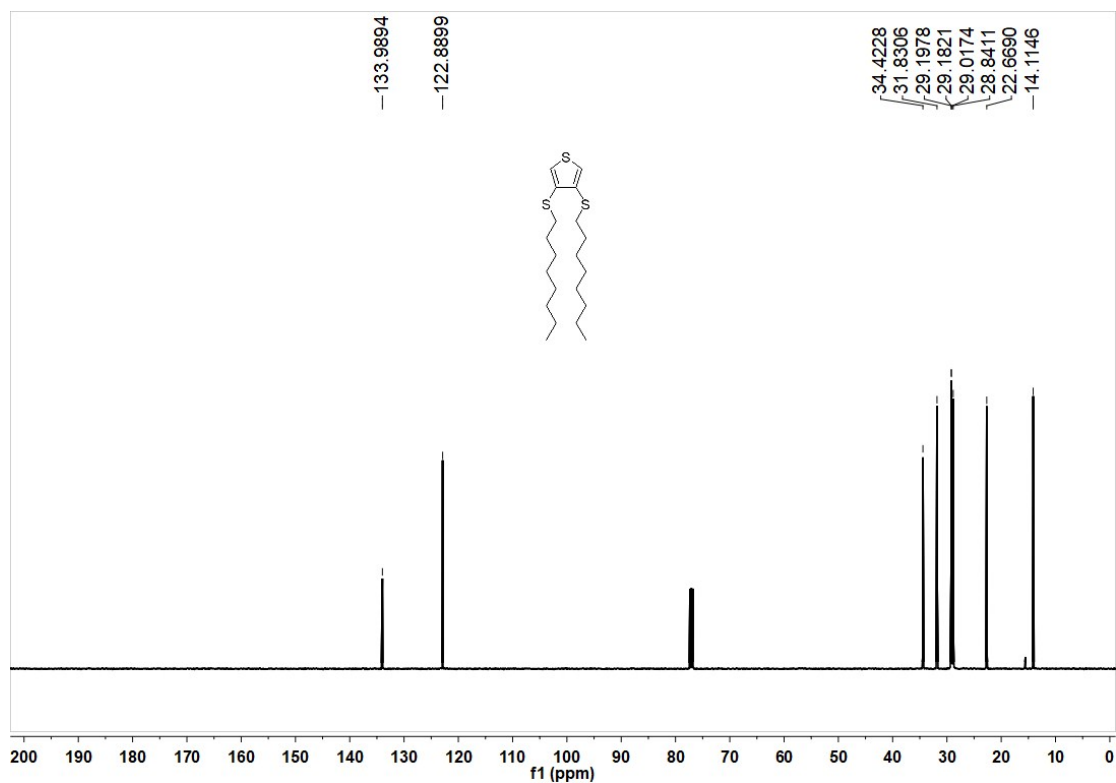


Fig. S2 ^{13}C NMR spectrum of compound 2.

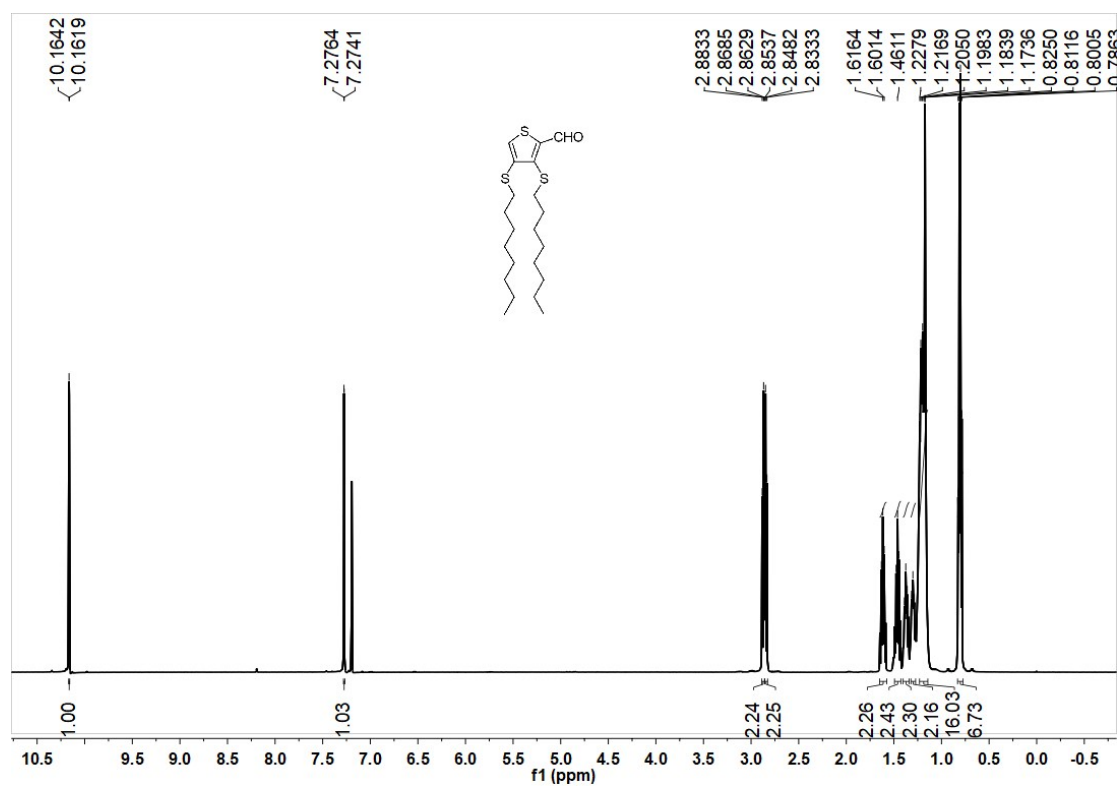


Fig. S3 ^1H NMR spectrum of compound 3.

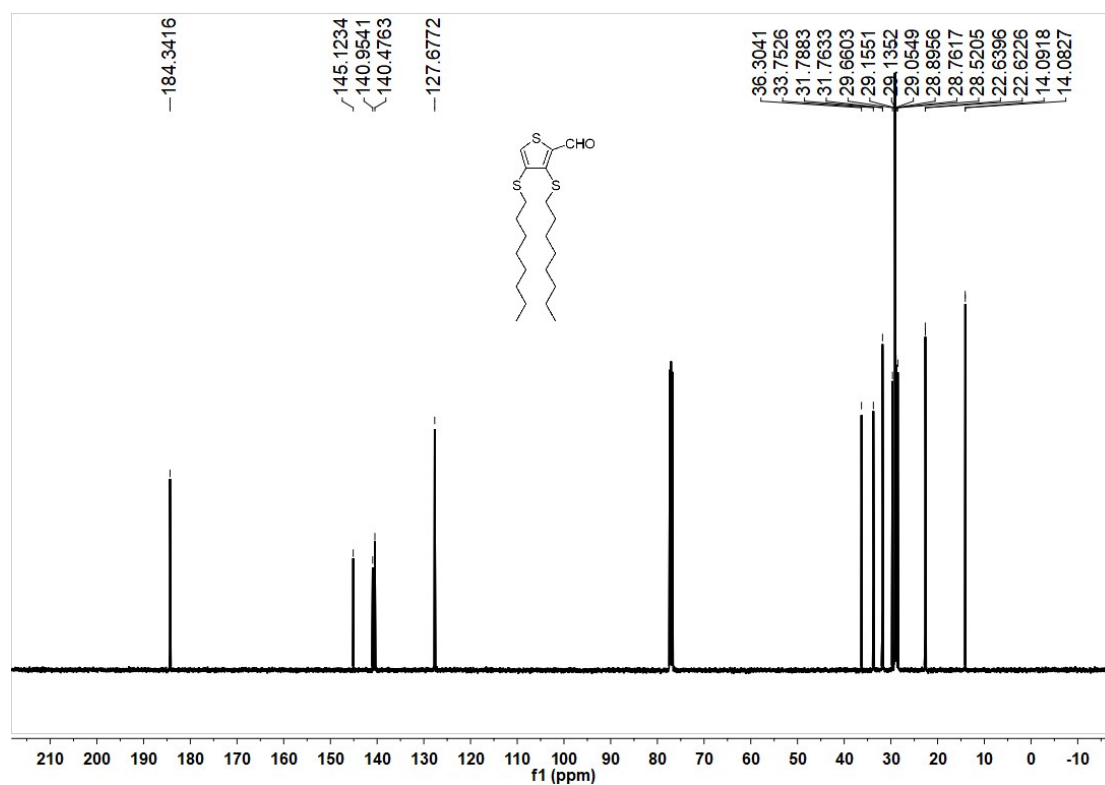


Fig. S4 ^{13}C NMR spectrum of compound 3.

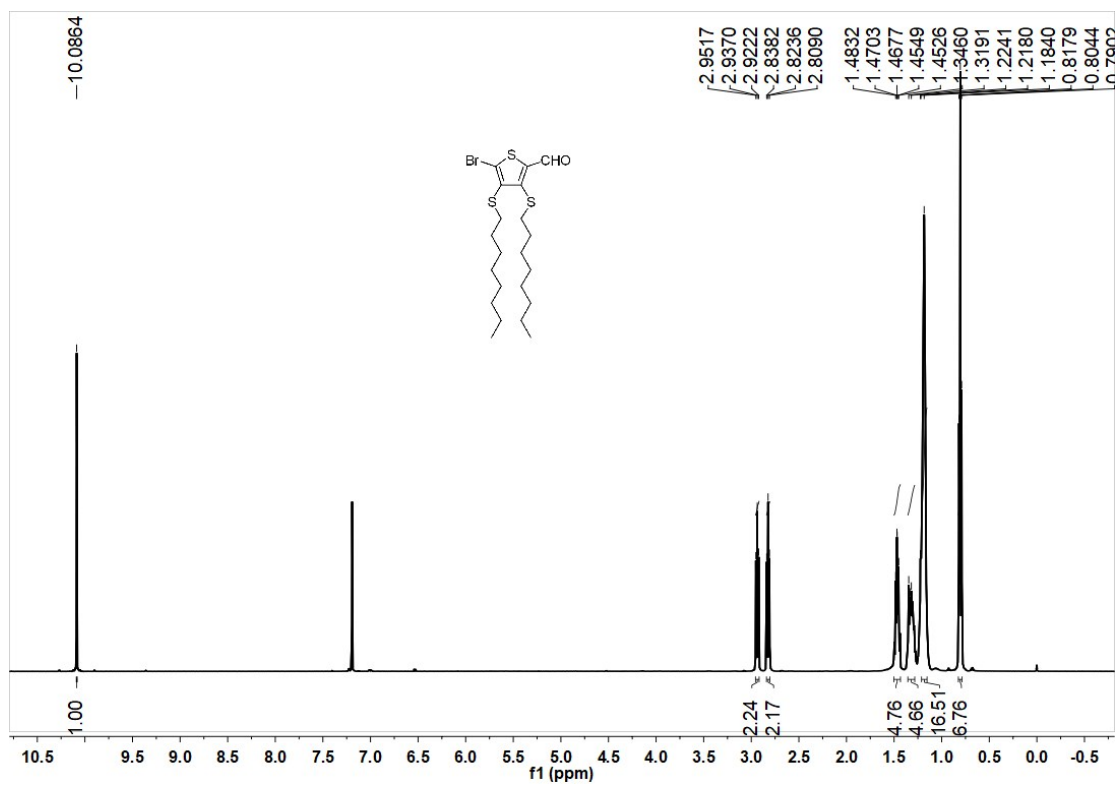


Fig. S5 ^1H NMR spectrum of compound 4.

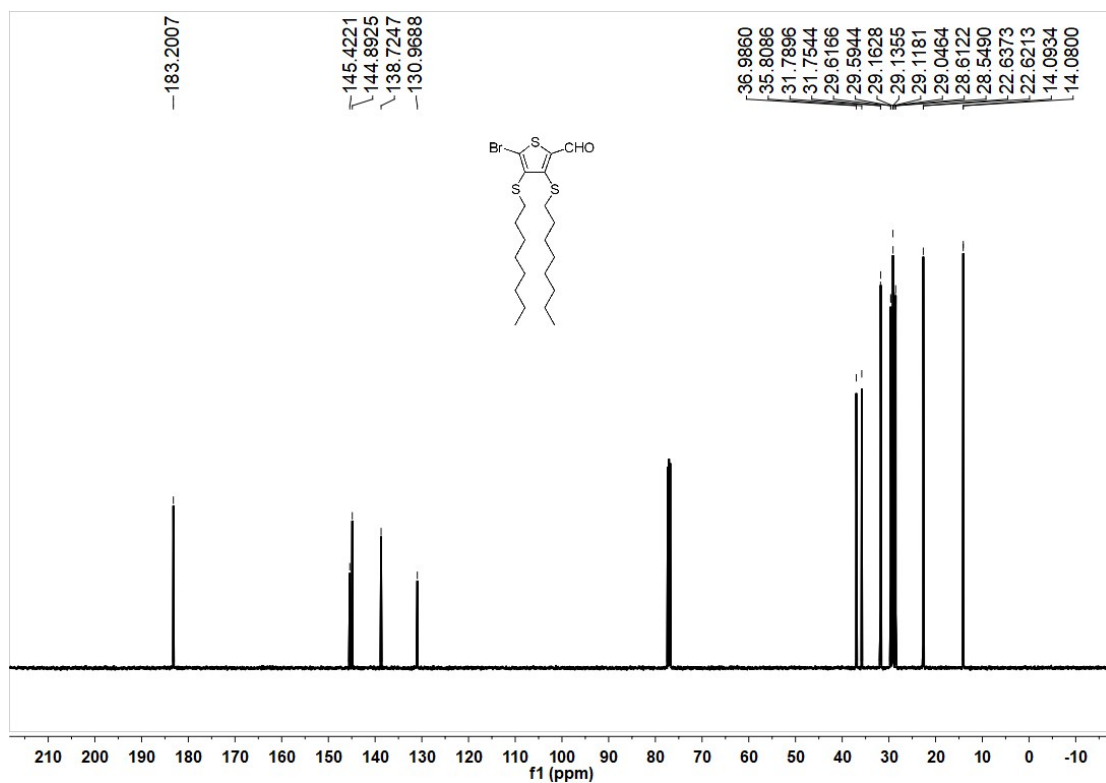


Fig. S6 ^{13}C NMR spectrum of compound 4.

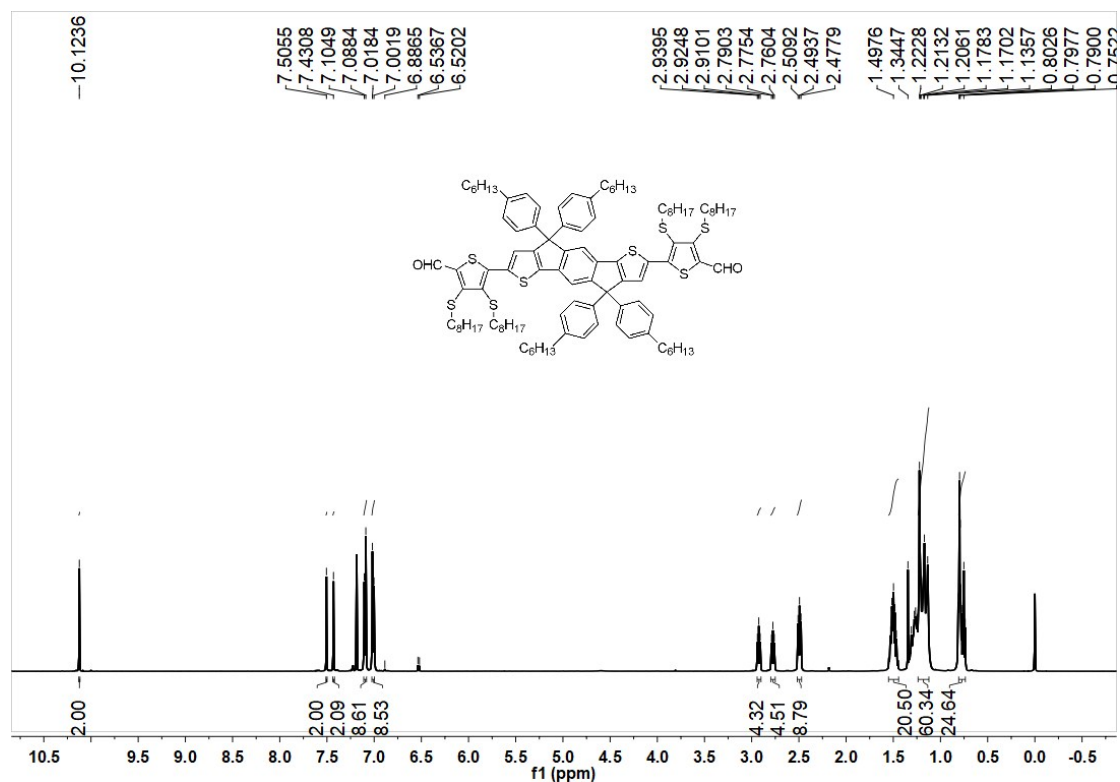


Fig. S7 ¹H NMR spectrum of compound 6.

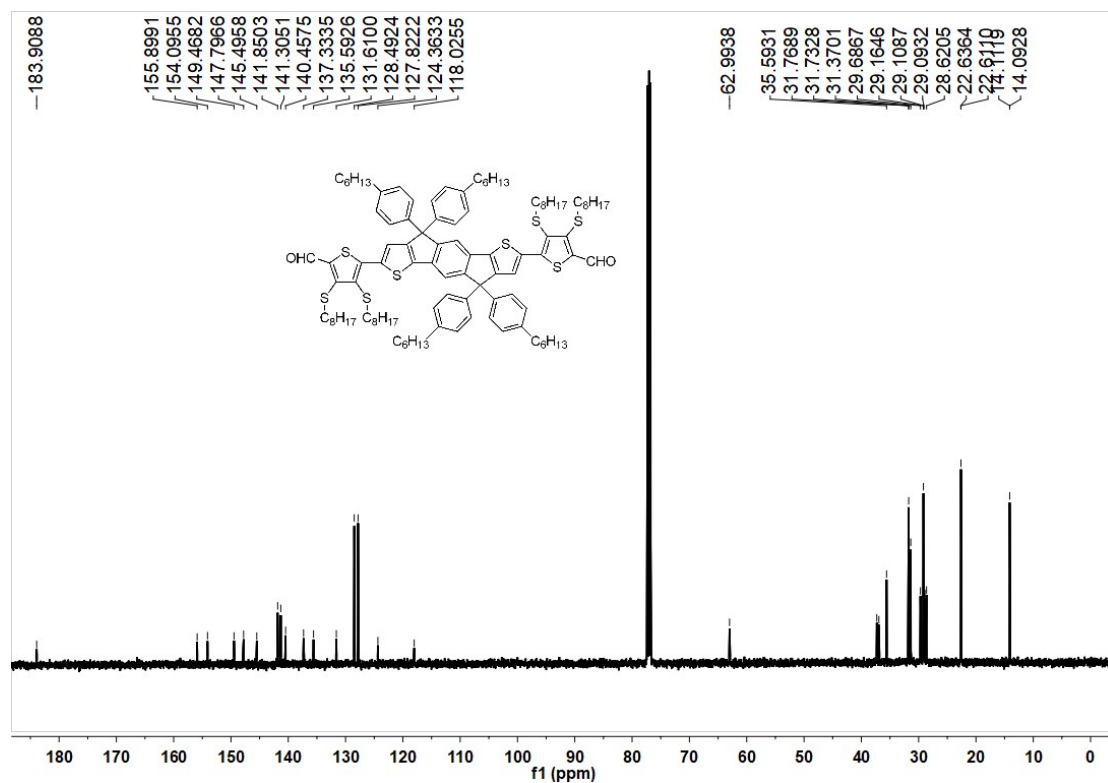


Fig. S8 ¹³C NMR spectrum of compound 6.

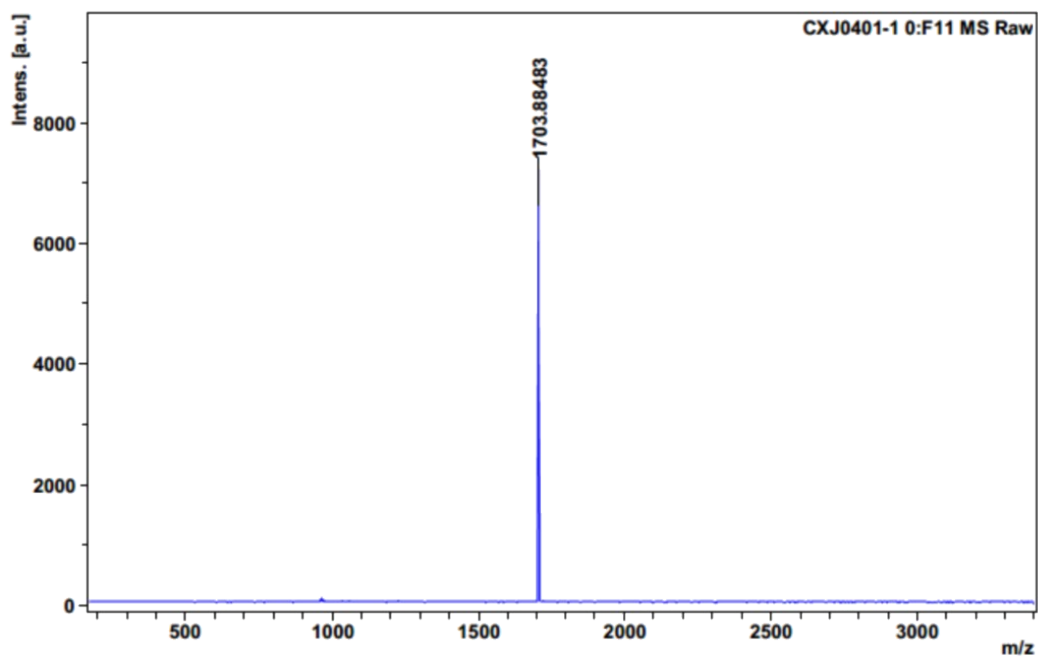


Fig. S9 MALDI-TOF mass spectrum of compound 6.

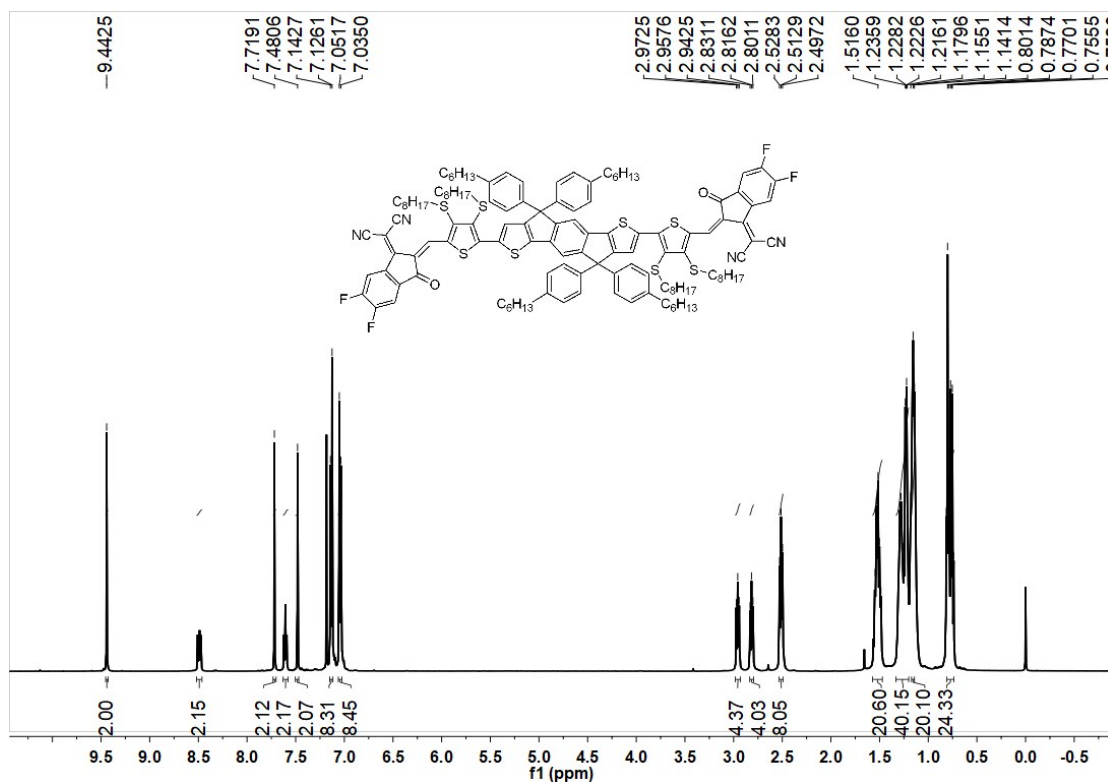


Fig. S10 ¹H NMR spectrum of IDT2ST-4F.

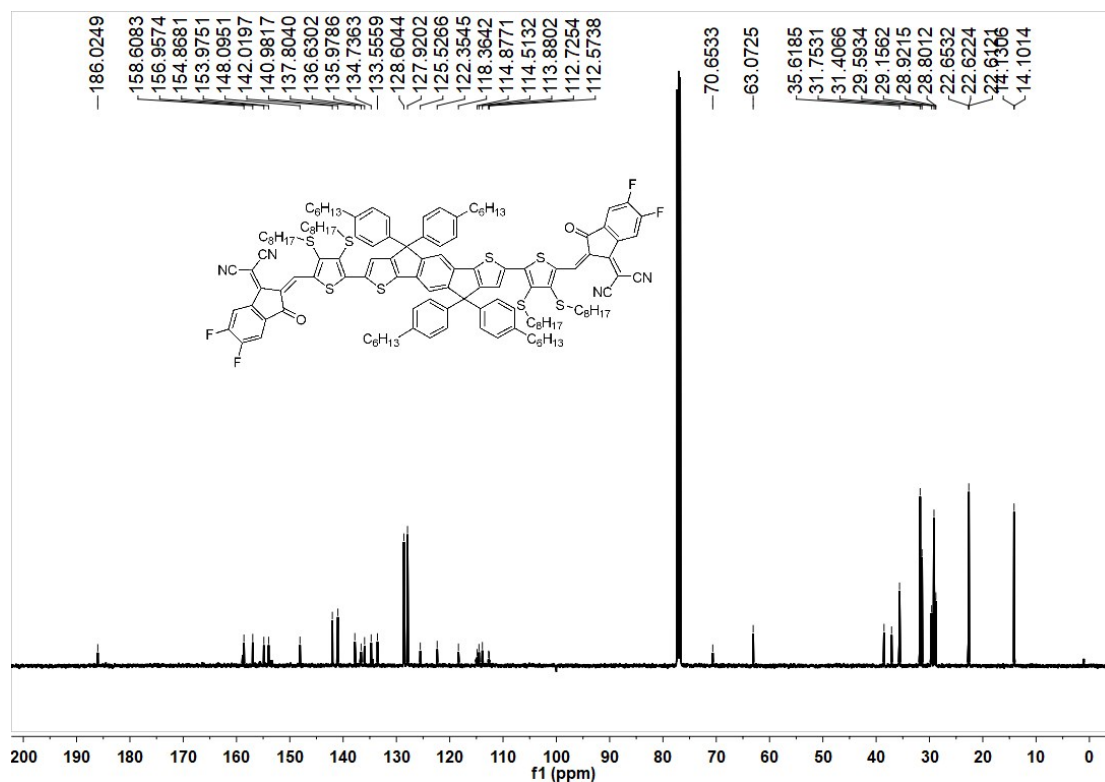
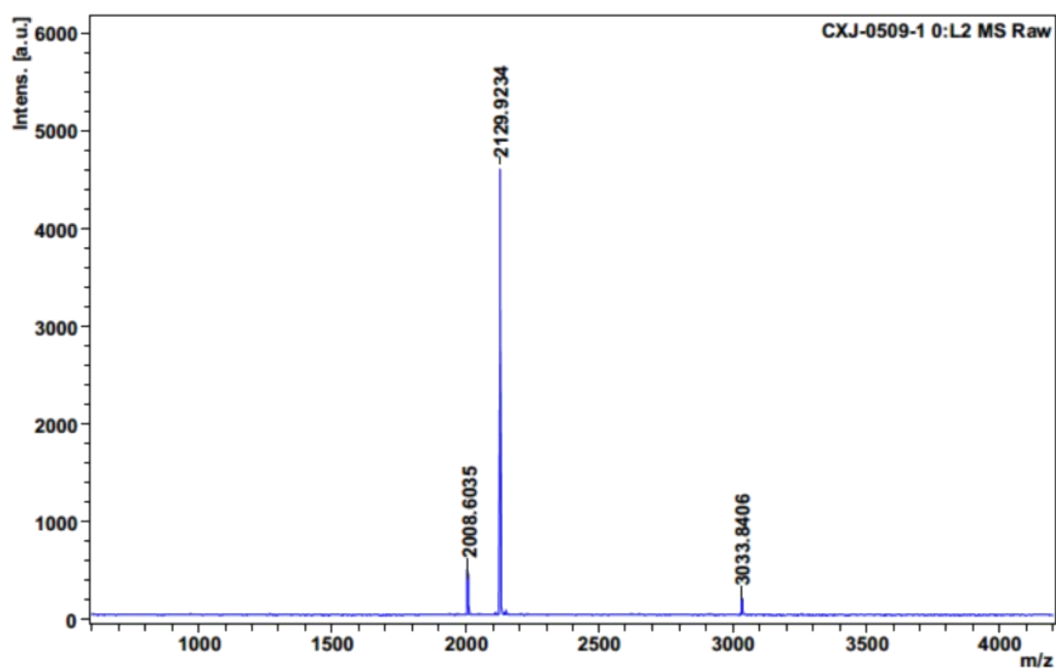


Fig. S11 ¹³C NMR spectrum of IDT2ST-4F.



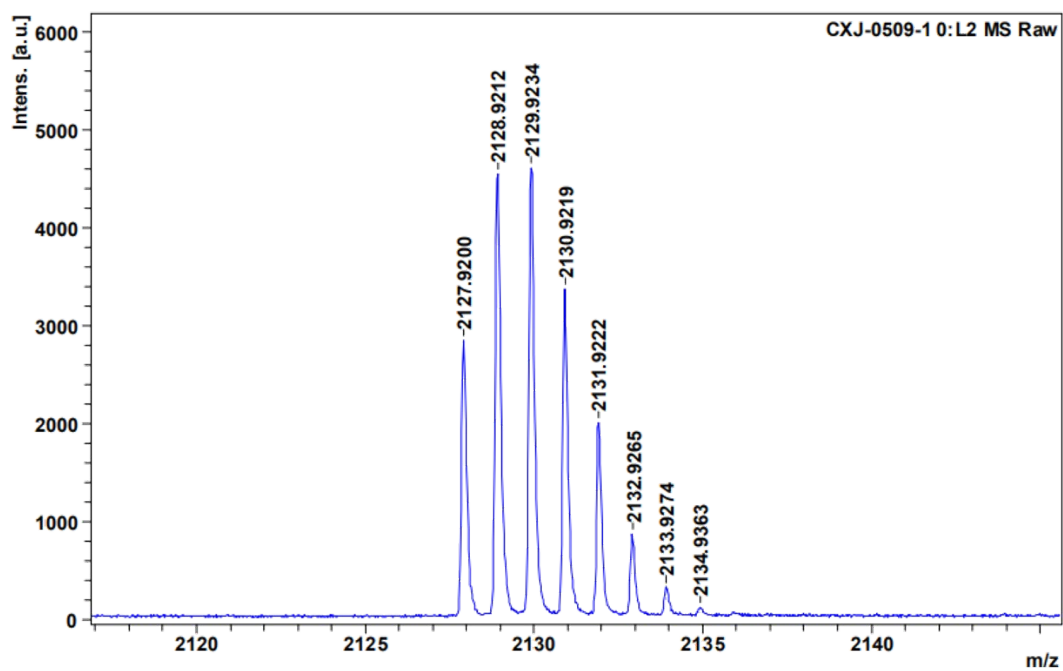


Fig. S12 MALDI-TOF mass spectrum of IDT2ST-4F.

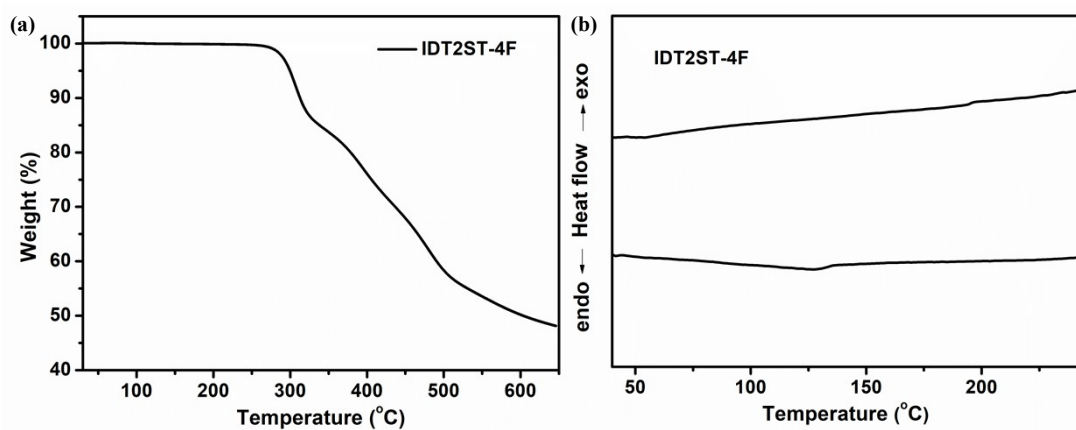


Fig. S13 (a) TGA and (b) DSC curves of IDT2ST-4F.

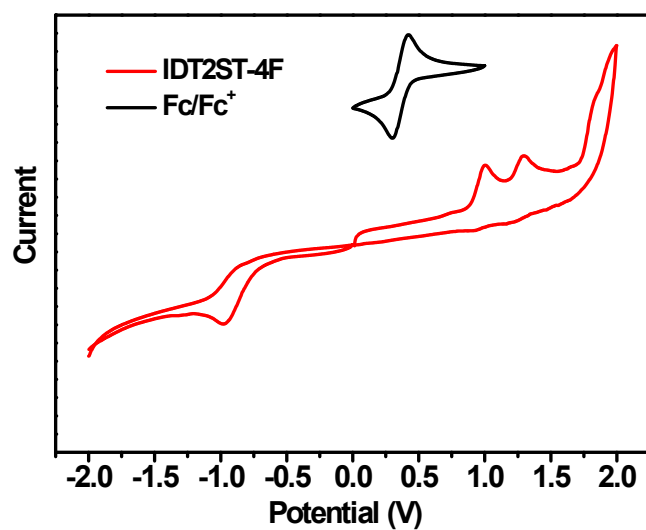


Fig. S14 Cyclic voltammogram of IDT2ST-4F in dichloromethane with 0.1 mol L⁻¹ n-Bu₄NPF₆ at a scan rate of 100 mVs⁻¹.

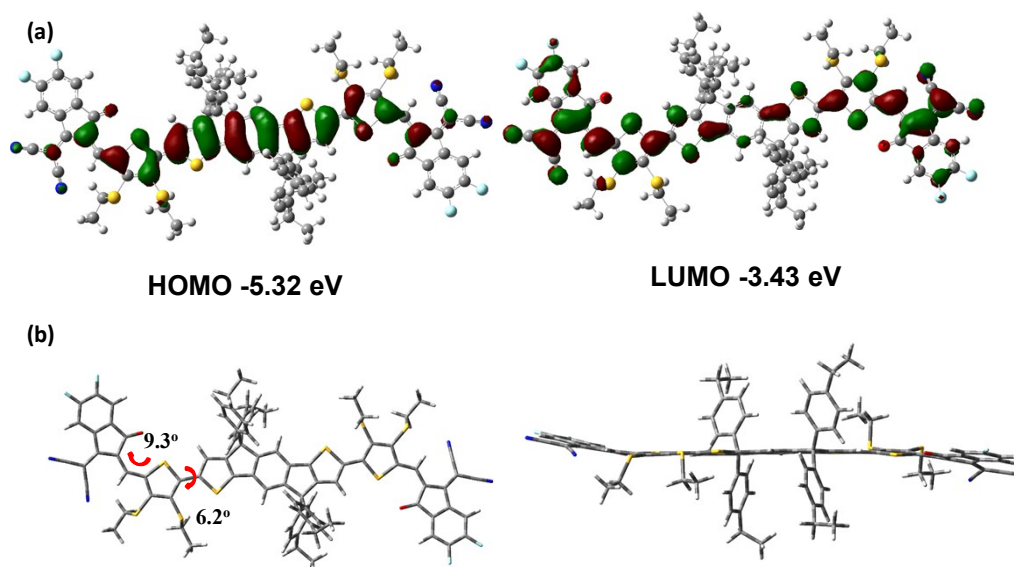


Fig. S15 (a) Electron density distributions of HOMO and LUMO orbitals, and (b) the optimized geometry of IDT2ST-4F with ethyl groups in replacing alkyl substituents to simplify the calculations.

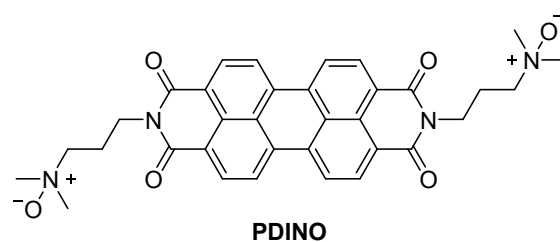


Fig. S16 Chemical structure of PDINO.

Photovoltaic performance

Table S1 Photovoltaic parameters of PBDB-T:IDT2ST-4F based devices with donor/acceptor weight ratio of 1:1 with thermal annealing at different temperatures for 5 min. The film thickness is about 100 nm and the solvent is chlorobenzene.

Conditions	V_{oc} (V)	J_{sc} (mA/cm ²)	FF (%)	PCE (%)
As-cast	0.854	17.32	62.6	9.27
100 °C	0.845	18.92	67.8	10.87
110 °C	0.849	19.44	69.3	11.43
120 °C	0.843	18.73	67.7	10.69
130 °C	0.838	18.36	69.0	10.50
140 °C	0.829	18.44	67.5	10.24

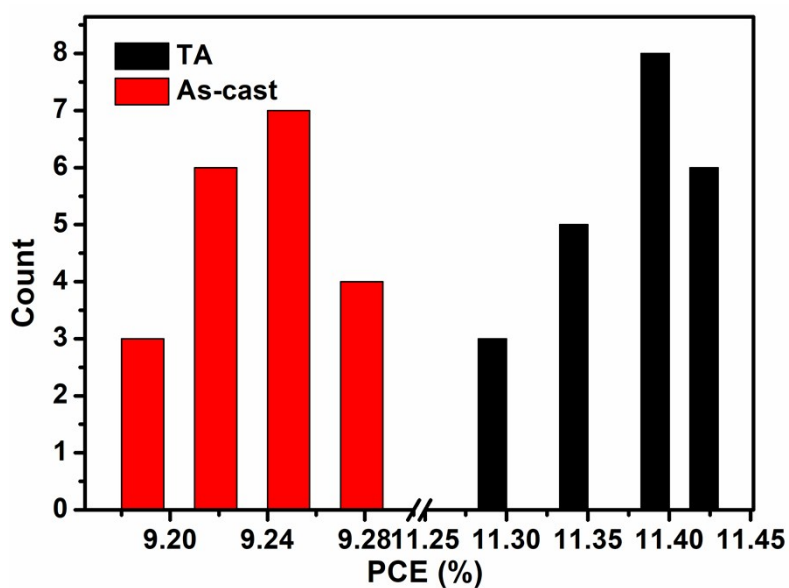


Fig. S17 Statistical histogram of PCEs for IDT2ST-4F-based devices (over 20 devices for each case under the as-cast or TA-treated conditions).

Table S2 Summary of the photovoltaic parameters of devices based on the IDT-cored small molecule acceptors.

Acceptor	E_g (eV)	Donor	V_{oc} (V)	J_{sc} (mA cm ⁻²)	FF (%)	PCE (%)	Ref
IDTT2F	1.46	PBDB-T	0.81	18.51	59	8.85	2
IDTCN-S	1.48	PBDB-T	0.85	19.04	65.7	10.60	3
ACS8	1.30	PTB7-Th	0.75	25.3	69.3	13.2	4
IEICO-4F	1.24	PBDB-T	0.77	20.10	56	8.66	5
IDTCN-O	1.53	PBDB-T	0.91	19.96	73.2	13.28	3
ITOIC-2F	1.45	PBDB-T	0.897	21.04	64.5	12.17	6
IDT2ST-4F	1.43	PBDB-T	0.849	19.44	69.3	11.43	<i>This work</i>

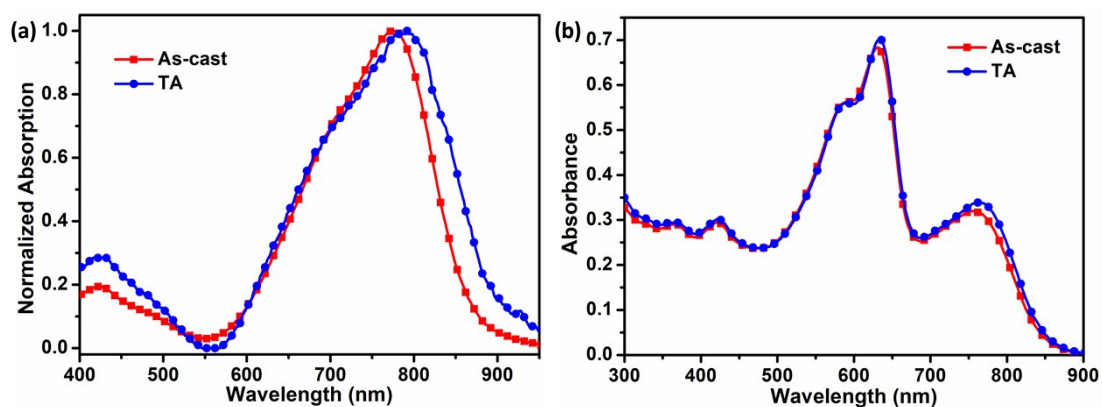


Fig. S18 Absorption spectra of the as-cast or TA-treated pristine IDT2ST-4F films (a) and PBDB-T:IDT2ST-4F films (b).

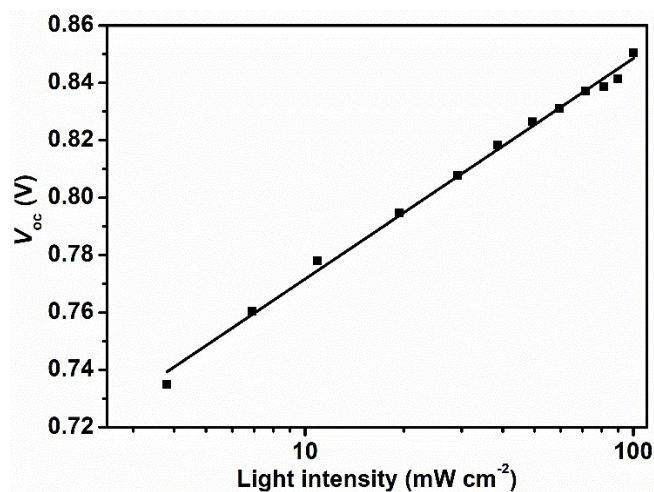


Fig. S19 Dependence of V_{oc} on the light intensity (P_{light}) of the TA-treated IDT2ST-4F-based devices.

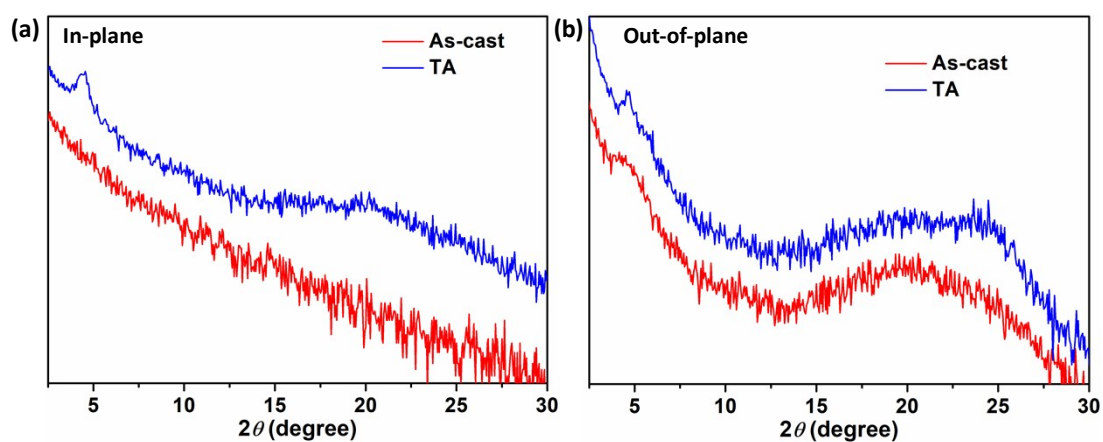


Fig. S20 (a) In-plane and (b) out-of-plane XRD pattern of the as-cast and TA-treated IDT2ST-4F film.

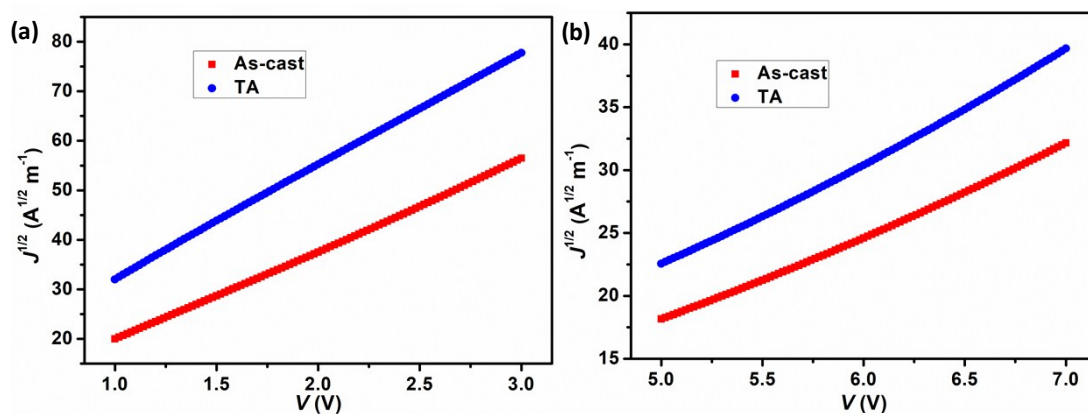


Fig. S21 J - V characteristics of the hole-only (a) and electron-only (b) devices based on the PBDB-T:IDT2ST-4F blend films under different conditions.

References

1. C. Sakong, S. H. Kim, S. B. Yuk, J. W. Namgoong, S. W. Park, M. J. Ko, D. H. Kim, K. S. Hong, J. P. Kim, *Chem. Asian J.* 2012, **7**, 1817-1826.
2. Y. Liu, M. Li, X. Zhou, Q.-Q. Jia, S. Feng, P. Jiang, X. Xu, W. Ma, H.-B. Li and Z. Bo, *ACS Energy Lett.*, 2018, **3**, 1832-1839.
3. Y. Liu, M. Li, J. Yang, W. Xue, S. Feng, J. Song, Z. Tang, W. Ma and Z. Bo, *Adv. Energy Mater.*, 2019, **9**, 1901280.
4. J. Chen, G. Li, Q. Zhu, X. Guo, Q. Fan, W. Ma and M. Zhang, *J. Mater. Chem. A*, 2019, **7**, 3745-3751.
5. H. Yao, Y. Cui, R. Yu, B. Gao, H. Zhang and J. Hou, *Angew. Chem. Int. Edit.*, 2017, **56**, 3045-3049.
6. Y. Liu, C. Zhang, D. Hao, Z. Zhang, L. Wu, M. Li, S. Feng, X. Xu, F. Liu, X. Chen and Z. Bo, *Chem. Mater.*, 2018, **30**, 4307-4312.